Proton diffusion pathways and rates in Y-doped $BaZrO_3$ solid oxide electrolyte from quantum mechanics

Boris Merinov[a] and William Goddard III
Materials and Process Simulation Center (139-74), California Institute of Technology, Pasadena, California 91125, USA

(Received 23 October 2008; accepted 19 March 2009; published online 20 May 2009)

We carried out quantum mechanical calculations (Perdew-Becke-Ernzerhof flavor of density functional theory) on 12.5% Y-doped $BaZrO_3$ (BYZ) periodic structures to obtain energy barriers for intraoctahedral and interoctahedral proton transfers. We find activation energy (E_a) values of 0.48 and 0.49 eV for the intraoctahedral proton transfers on O–O edges (2.58 and 2.59 Å) of ZrO_6 and YO_6 octahedra, respectively, and E_a=0.41 eV for the interoctahedral proton transfer at O–O separation of 2.54 Å. These results indicate that both the interoctahedral and intraoctahedral proton transfers are important in the BYZ electrolyte. Indeed, the calculated values bracket the experimental value of E_a=0.44 eV. Based on the results obtained, the atomic level proton diffusion mechanism and possible proton diffusion pathways have been proposed for the BYZ electrolyte. The thermal librations of BO_6 octahedra and uncorrelated thermal vibrations of the two oxygen atoms participating in the hydrogen bond lead to a somewhat chaotic fluctuation in the distances between the O atoms involved in the hydrogen bonding. Such fluctuations affect the barriers and at certain O–O distances allow the hydrogen atoms to move within the hydrogen bonds from one potential minimum to the other and between the hydrogen bonds. Concertation of these intra- and inter-H-bond motions results in *continuous* proton diffusion pathways. Continuity of proton diffusion pathways is an essential condition for fast proton transport. © *2009 American Institute of Physics*. [DOI: 10.1063/1.3122984]

I. INTRODUCTION

Perovskite oxides are very important technological materials with a number of interesting physicochemical properties, including high-temperature superconductivity, ferroelectricity, piezoelectricity, colossal magnetoresistance, and catalytic and transport properties. In particular acceptor-doped perovskite-type oxides exhibit high protonic conductivity at elevated temperatures, when they are exposed to water vapor.[1–6] This allows a greatly reduced operating temperature compared to that for commercial solid oxide fuel cells based on yttria-stabilized zirconia. In addition, doped perovskite oxides often exhibit very good chemical and mechanical stabilities, making them attractive for potential applications in such electrochemical devices as fuel cells, hydrogen sensors, and hydrogen pumps.

In most solid oxide proton conductors the principal features of the proton transport mechanism are generally described as the two-step Grotthuss-type diffusion mechanism, which consists of

(1) fast rotational diffusion of a $[OH_O^{\bullet}]$ protonic defect (the hydroxide ion at the oxygen site), and
(2) proton transfer within a hydrogen bond between two neighboring BO_6 octahedra (interoctahedral proton transfer) or between two oxygen atoms belonging to the same BO_6-octahedron (intraoctahedral proton transfer).[7]

Experimental and theoretical results both show that the rotational diffusion occurs with a low activation barrier in most studied proton-conducting perovskite oxides and that the proton transfer is often a rate-limiting step in the proton transport mechanism.[7,8] The energy barrier for proton transfer is assumed to contribute significantly to the activation energy of the proton conductivity. Experimentally, it is difficult to determine proton migration pathways and energy barriers. Thus we use quantum mechanics (QM) methods [density functional theory (DFT)] to examine the atomic-scale proton movements. To do this we model the proton movements in a supercell, obtained by repeating the unit cell for the ideal nondefected structure, and then calculate the energy barriers for various proton migration pathways.

In this paper we will focus on Y-doped $BaZrO_3$ (BYZ), known as one of the most promising proton-conducting ceramics. Here we assume that each Y substitution leads also to an extra proton. Although this work is a part of our efforts on development of a first-principles-based ReaxFF reactive force field for materials and processes suitable for oxygen- and proton-conducting solid oxide fuel cells,[9,10] we believe that the obtained QM result itself is valuable. Previous computational works reported either too low [0.25 eV, conjugate gradient minimizations and nudged elastic band (NEB) calculations[11]], or too high values (0.83 eV, quantum molecular dynamics simulations[12]) for the proton transfer activation energy in BYZ in comparison to experimental value of 0.44 eV. The noticeable difference and the large range for the calculated activation energy required further computa-

[a]Author to whom correspondence should be addressed. Electronic mail: merinov@wag.caltech.edu. FAX: +1-626-585-0918.

tional work to better describe the proton diffusion energetics in BYZ. Our computational approach provides much better agreement with experiment. Other aspects of the proton diffusion in BYZ are also discussed in the paper.

II. COMPUTATIONAL TECHNIQUES

A. Quantum mechanics

All QM calculations were performed at $T=0$ K using DFT with Perdew-Becke-Ernzerhof (PBE)[13] flavor of the generalized gradient approximation.[14,15] We applied the SEQQUEST (Ref. 16) periodic DFT code that employs contracted Gaussian basis sets rather than plane waves. The core electrons of Ba, Y, Zr, and O atoms were replaced with an effective core potential (pseudopotentials) in which angular momentum projection operators were used to replace the core electrons and to enforce the Pauli principle[17] and for which the long-range atomic orbital amplitudes are preserved (norm conserving).[18] The basis sets were optimized at the double zeta plus polarization contracted level. A $4\times4\times4$ reciprocal space grid (k-points) was used for the QM calculations.

B. The super cell model

The protonic defect was modeled in a BYZ supercell composed of eight primitive cubic BYZ unit cells. The lattice parameters of the supercell and atomic coordinates were allowed to relax for the initial $Ba_8Zr_7YHO_{24}$ structure.

We expected that the barriers for the intraoctahedral and interoctahedral proton transfers would depend on the lengths of the corresponding hydrogen bonds, the O–O edge of the BO_6 octahedron and the O–O distance between two neighboring BO_6 octahedra. Thus we investigated this dependence using

(1) 2.69, 2.58, 2.50, and 2.46 Å for the intraoctahedral O–O edge of the ZrO_6-octahedron in the Zr-OH-Y configuration, and 2.88, 2.69, 2.56, and 2.45 Å in the Zr-OH-Zr configuration,
(2) 2.89, 2.75, 2.59, and 2.43 Å for the intraoctahedral O–O edge of the YO_6-octahedron, and
(3) 3.07, 2.79, 2.71, 2.62, 2.54, and 2.46 Å for the interoctahedral O–O distance.

For each distance we fixed the corresponding oxygen atoms and allowed all other atoms and the lattice parameters to relax. Since at the proton transfer within the hydrogen bond each oxygen atom participating in formation of the hydrogen bond can switch from a proton donor to a proton acceptor, we optimized the two "ending" structures with the hydrogen atom close to the one oxygen atom and to the other for each case. Then for each case the barriers were calculated by stepwise movement of the hydrogen atom from the one oxygen to the other. In these barrier calculations all atoms and lattice parameters were fixed. We used the appropriate ending structure for the halfway point of the proton transfer. This approach led to reasonable shapes of the barriers, making reasonably symmetrical.

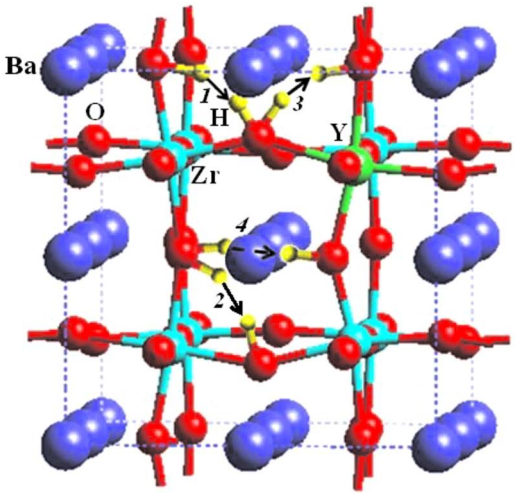

FIG. 1. (Color online) Proton transfer in BYZ. (1) Intra-ZrO_6-octahedral proton transfer in the Zr–OH–Y configuration. (2) Intra-ZrO_6-octahedral proton transfer in the Zr–OH–Zr configuration. (3) Intra-YO_6-octahedral proton transfer. (4) Interoctahedral proton transfer between two neighboring BO_6 octahedra.

III. RESULTS AND DISCUSSION

A. Barriers for intra-(ZrO_6)-octahedral proton transfer

We started by investigating the energy barrier for the intraoctahedral proton transfer on the edge of a distorted ZrO_6-octahedron. There exist two different configurations for this type of the intraoctahedral proton transfer. The first one is Zr–OH–Y, in which the neighboring polyhedra are a ZrO_6-octahedron and YO_6-octahedron, and the second configuration is Zr–OH–Zr, that is the neighboring polyhedra are ZrO_6 octahedra (Fig. 1). According to our calculations the Zr–OH–Y configuration is more stable (by 0.24 eV) than the Zr–OH–Zr one. This is in agreement with results obtained in Ref. 19. We also found that in both cases the proton transfer barriers depend significantly on the length of the O–O edge.

In the initial completely relaxed $Ba_8Zr_7YHO_{24}$ structure (the ground state) the H-bonded edge of the ZrO_6-octahedron in the Zr–OH–Y configuration has $O-O=2.69$ Å, while lengths of all other edges vary from 2.96 to 3.14 Å. The short O–O edge of the ZrO_6-octahedron is probably possible due to having a larger YO_6-octahedron as a neighbor. Our calculation of a proton transfer barrier on this 2.69 Å O–O edge leads to a value of 0.76 eV (Table I), which is in good agreement with 0.83 eV for a 2.72 Å O–O edge obtained using quantum molecular dynamics in Ref. 12.

Decreasing the O–O edge to 2.58 Å results in a significantly lower proton transfer barrier of 0.48 eV, but the overall energy increase due to the structure distortion is only 0.06 eV. Thus the net barrier (sum of both contributions) is reduced to 0.54 eV.

Further decreasing the O–O edge to 2.50 Å leads to a proton transfer barrier of 0.34 eV, while the structure distortion contribution increases to 0.14 eV. Thus the net barrier is reduced further to 0.48 eV, which is very close to the experimentally observed value of 0.44 eV.[4]

At the O–O separation of 2.46 Å there is almost no

TABLE I. Relative energetic contributions to the activation energy for the intraoctahedral proton transfer resulting from the change of the O–H···O hydrogen bond geometry.

O–O edge (Å)	O–H (Å)	H···O (Å)	$\angle O_D HO_A$ (deg)	B–O_D (Å)	B–O_A (Å)	B–H (Å)	Proton transfer barrier (eV)	Structure distortion contribution (eV)	Sum of contributions (eV)
					ZrO_6-octahedron, Zr–OH–Y configuration				
2.69	1.00	1.85	139.86	2.34	2.10	2.30	0.76		0.76
2.58	1.01	1.68	145.24	2.32	2.15	2.25	0.48	0.06	0.54
2.50	1.02	1.60	145.60	2.25	2.17	2.22	0.34	0.14	0.48
2.46	1.03	1.52	147.81	2.23	2.21	2.21	0.08	0.24	0.32
					ZrO_6-octahedron, Zr–OH–Zr configuration				
2.88	0.98	2.13	131.59	2.31	2.21	2.34	1.35	0.24	1.59
2.69	1.00	1.83	142.75	2.26	2.32	2.29	0.76	0.34	1.10
2.56	1.01	1.63	150.24	2.20	2.45	2.25	0.34	0.60	0.94
2.45	1.05	1.44	158.91	2.15	2.64	2.25	0.10	1.01	1.11
					YO_6-octahedron				
2.89	0.99	2.09	136.76	2.32	2.27	2.35	1.23	0.03	1.26
2.75	0.99	1.89	142.54	2.30	2.28	2.30	0.84	0.05	0.89
2.59	1.01	1.66	150.10	2.30	2.29	2.25	0.31	0.18	0.49
2.43	1.04	1.45	155.32	2.29	2.31	2.22	0.10	0.24	0.34

barrier (~0.08 eV) for the proton transfer, but the structure distortion increases to 0.24 eV. Thus the net barrier is reduced further to 0.32 eV.

The H-bonded edge in the Zr–OH–Zr configuration has O–O=2.88 Å (Fig. 1) and the calculated proton transfer barrier on this edge is 1.35 eV (Table I), significantly higher than on the H-bonded edge of the ZrO_6-octahedron in the Zr–OH–Y configuration, 0.76 eV. The structure distortion contribution is 0.24 eV.

Decreasing the O–O edge to 2.69 Å leads to a lower proton transfer barrier of 0.76 eV, whereas the energy increase due to the structure distortion becomes 0.34 eV. Thus the net barrier is still quite high, 1.10 eV. Further decreasing the O–O edge to 2.56 Å results in a proton transfer barrier of 0.34 eV, while the structure distortion contribution increases to 0.60 eV. Thus the net barrier is reduced to 0.94 eV, but nevertheless it remains significantly higher than the experimentally observed value of 0.44 eV.[4]

At the very short O–O separation of 2.45 Å a very low barrier of 0.10 eV is obtained for the proton transfer, but the structure distortion contribution becomes very high, 1.01 eV. Thus the net barrier is 1.11 eV, even higher than that for the O–O edge of 2.56 Å.

All above net barriers for the Zr–OH–Zr configuration are significantly higher than the experimentally observed activation energy, 0.44 eV.[4] Therefore, the probability of the proton transfer on the O–O edge of the ZrO_6-octahedron in the Zr–OH–Zr configuration is much lower than on the O–O edges of the ZrO_6 and YO_6 octahedra in the Zr–OH–Y configurations.

B. Barriers for intra-(YO_6)-octahedral proton transfer

We have also examined the proton transfer along the O–O edge of the YO_6-octahedron (Fig. 1). The energy of the completely relaxed $Ba_8Zr_7YHO_{24}$ structure with hydrogen on the edge of the YO_6-octahedron is only 0.03 eV higher than that of the ground structure with hydrogen on the edge of the ZrO_6-octahedron in the Zr–OH–Y configuration. The O–O edges of the YO_6-octahedron are longer than the O–O edges of the ZrO_6-octahedron. The H-bonded O–O=2.89 Å, which is very close to the H-bonded O–O edge (2.88 Å) of the ZrO_6-octahedron in the Zr–OH–Zr configuration, but significantly longer than that of the ZrO_6-octahedron in the Zr–OH–Y configuration, 2.69 Å. The other O–O edges of the YO_6-octahedron are going up to 3.31 Å. The proton transfer barrier is 1.23 eV, lower than 1.35 eV on the edge of the ZrO_6-octahedron in the Zr–OH–Zr configuration, but significantly higher than on the edge of the ZrO_6-octahedron in the Zr–OH–Y configuration, 0.76 eV (Table I).

Decreasing the O–O edge again drastically lowers the proton transfer barrier. Thus for O–O=2.59 Å the barrier becomes 0.31 eV, while the corresponding structure distortion contribution is only 0.18 eV. This leads to a total activation energy of 0.49 eV which is close to the experimentally observed activation energy of 0.44 eV. For the ZrO_6-octahedron in the Zr–OH–Y configuration similar values for the proton transfer barrier and activation energy are reached at the shorter O–O distance of 2.50 Å. These results indicate that the barrier for intraoctahedral H migration is not only a function of the O–O distance, but also depends on a metal involved. The intraoctahedral proton transfer may occur on edges of the YO_6 octahedra at longer O–O distances (<2.59 Å) than on the ZrO_6 octahedra (<2.50 Å). Probably at least partly this is due to a weaker electrostatic repulsion between a trivalent Y dopant atom and a proton compared with that between a tetravalent Zr atom and a proton.

For an O–O edge of 2.43 Å of the YO_6-octahedron the barrier for the proton transfer decreases to 0.10 eV, while the contribution from structure distortion is 0.24 eV, leading to an overall contribution to the activation energy of 0.34 eV.

TABLE II. Relative energetic contributions to the activation energy for the interoctahedral proton transfer resulting from the change of the O–H···O hydrogen bond geometry between BO_6 octahedra.

O–O edge (Å)	O–H (Å)	H···O (Å)	∠OHO (deg)	Proton transfer barrier (eV)	Structure distortion contribution (eV)	Sum of contributions (eV)
3.07	0.99	2.08	179.32	1.26	0.09	1.35
2.79	1.01	1.79	179.37	0.59	0.13	0.72
2.71	1.01	1.69	179.42	0.41	0.16	0.57
2.62	1.03	1.60	179.45	0.25	0.21	0.46
2.54	1.04	1.50	179.34	0.13	0.28	0.41
2.46	1.07	1.38	179.20	0.04	0.38	0.42

These values are very similar to those for an O–O edge of 2.46 Å of the ZrO_6-octahedron in the Zr-OH-Y configuration (see Table I).

C. Barriers for interoctahedral proton transfer

In addition to the intraoctahedral proton transfer we have examined proton hopping between oxygen atoms that belong to adjacent BO_6 octahedra (Fig. 1), referred to as interoctahedral proton transfer. Here we optimized the $Ba_8Zr_7YHO_{24}$ structure with the hydrogen in between two adjacent BO_6 octahedra, finding an O–H···O distance of 3.07 Å in the completely relaxed structure. For this distance the calculated energy barrier for the interoctahedral hydrogen transfer is 1.26 eV, while the energy of the overall given structure increases by 0.09 eV compared to the energy of the ground structure. The sum of both contributions is 1.35 eV (Table II), which is significantly higher than that for the intraoctahedral proton transfer.

However, decreasing the O–H···O distance to 2.79 Å abates the energy barrier to 0.59 eV, whereas the total energy of the overall structure increases only by 0.04 eV. Further decreasing the O–H···O distance to 2.54 Å leads to a proton transfer barrier of 0.13 eV and a structure distortion contribution of 0.28 eV. The sum of both contributions to the activation energy is 0.41 eV, in good agreement with the experimental value of 0.44 eV.

Decreasing the interoctahedral O–H···O bond to 2.46 Å, we find a proton transfer barrier of 0.04 eV, while the structure distortion contribution becomes equal to 0.38 eV. Hence, the sum of both contributions is 0.42 eV.

From the barriers calculated for the interoctahedral proton transfer, we can assume that perhaps this type of proton transfer also occurs in BYZ, although this conclusion would contrast with that in Refs. 11 and 12 which predict only intraoctahedral proton transfer in BYZ.

D. Proton diffusion mechanism

Based on the above results, we suggest the following atomic level mechanism and pathways for proton diffusion in the BYZ electrolyte. The thermal librations of the BO_6 octahedra and uncorrelated thermal vibrations of the two oxygen atoms participating in the hydrogen bond lead to a somewhat chaotic fluctuation in the distances between the O atoms involved in the hydrogen bonding. Occasionally the O–O distance will become short enough (~2.4–2.6 Å) that the potential barrier for the hydrogen atom to hop from one O to the other becomes low (see Tables I and II) and the proton has a probability to overcome the barrier to hop from one OH potential minimum to the other. This leads to *intra-H-bond motion*. The intra-H-bond motion is related to both intra- and interoctahedral proton transfers. On the other hand, due to the same thermal processes, the hydrogen bond can elongate so that the long (and weak) H···O-acceptor link of the existing hydrogen bond easily breaks and a new hydrogen bond forms with another oxygen-acceptor atom due to reorientation of the O–H-donor link—*inter-H-bond motion*. According to our calculations the barrier for such reorientation of the hydrogen bond is ~0.05 eV. Concertation of these intra- and inter-H-bond motions results in *continuous* proton diffusion pathways. This is an essential condition for successful proton transport.[20]

Let's assume that at some moment in time one of the hydrogen atoms occupies a position denoted by 0 in Fig. 2. As it was mentioned in Sec. III A, the probability of the proton transfer on the O–O edge of the ZrO_6-octahedron in the Zr–OH–Zr configuration is low due to the high net barrier. Thus, from this position the hydrogen atom can either jump into position 1 (the O–H-link reorientation) to form a

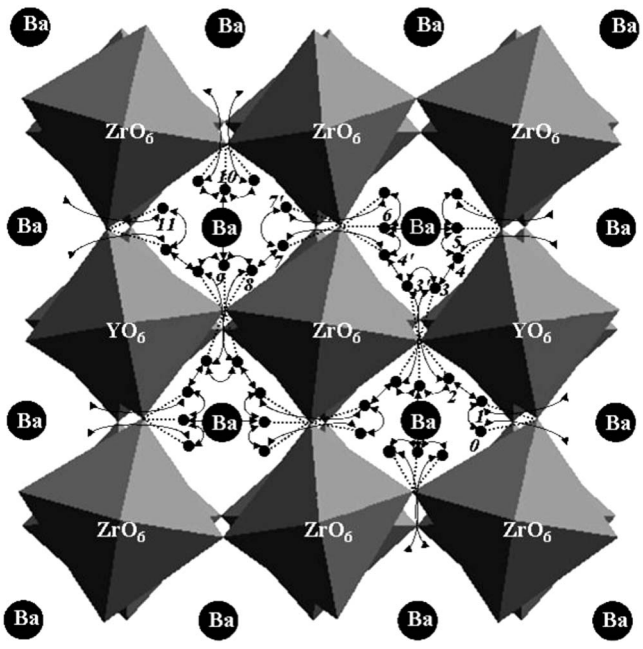

FIG. 2. Possible proton diffusion pathways in BYZ.

new hydrogen bond on the O–O edge of another BO_6-octahedron (inter-H-bond motion) or the O–H-link rotates as it shown by the longer arrow in Fig. 2. We will choose the jump into position 1. Even after jumping, the hydrogen atom may hop back into the previous position. Such local fluctuations forth and back (local diffusion) may befall at each step of a pathway and do not contribute to the long-range proton diffusion in BYZ. In order the long-range proton diffusion to occur the hydrogen atom must jump into a new position (position 2, intra-H-bond motion) and not return to the previous one. The next step might be a jump from position 2 to position 3 which can be considered as a rotation of the O–H-donor link of the hydrogen bond (inter-H-bond motion). From position 3 the proton hops to position 4 (intra-H-bond motion) and then to position 5 (inter-H-bond motion). Up until now all described steps occurred on the edges of the BO_6 octahedra and in a sense can be considered as intraoctahedral proton transfer. The further step, the intra-H-bond motion from position 5 to position 6, is interoctahedral proton transfer. This interoctahedral proton transfer becomes possible due to a particular orientation of the BO_6 octahedra, at which the O–O distance between the BO_6 octahedra is short enough to form the hydrogen bond. Position 6 can also be reached by the proton from position 3 through position 3′ (inter-H-bond motion) and position 4′ (intra-H-bond motion), and again the inter-H-bond motion from position 4′ to position 6. We will not discuss further possible steps (6–11, etc.) of the proton diffusion in BYZ because they are quite similar to steps 1–6 which have already been analyzed above. The proposed proton diffusion pathway is only one of lots. Some of them can easily be found using Fig. 2. For instance, the proton from position 2 could jump to some position lying out of the figure plane (one should remember that the experimentally observed symmetry of the BYZ structure is cubic and, hence, all three directions x, y, and z are equivalent) and, therefore, a new hydrogen bond in a plane perpendicular to the figure plane can be formed. In this case, it is possible that a number of further proton diffusion steps would generally occur in the plane perpendicular to the figure plane.

E. Comparison to previous computational results

Proton diffusion in this material was earlier theoretically investigated using DFT,[11,17] based on the plane-wave pseudopotential approach as implemented in the Vienna *ab initio* simulation package (VASP),[21] and quantum molecular dynamics.[12]

Gomez *et al.*[11] examined proton binding sites and minimum energy pathways between the binding cites in perovskite oxides including BYZ via conjugate gradient minimizations and the NEB method.[22] They found that the two most stable proton positions in BYZ (in our study these are initial positions for intra- and interoctahedral proton transfers) are very close in energy and rotation between them involves going over a very small barrier (less than 0.02 eV). We obtained a similar result with the barrier of ~0.05 eV. However, our value for the activation energy, 0.41 eV, is in much better agreement with the experimental activation energy of 0.44 eV, than 0.25 eV calculated by Gomez *et al.*[11] Such a low activation energy barrier was obtained in Ref. 11 because the authors used the NEB method that allows full relaxation of generated structural images between two minima on a potential energy surface. This full relaxation of the intermediate states most probably does not occur during the fast proton transfer process.

Björketun *et al.*[19] employed a jump-diffusion model[23] developed to describe proton transport in cubic perovskites. They found the migration barrier of 0.3 eV encountered by protonic defects trapped in the near-dopant region and the 0.2 eV barrier in the defect-free region. Although the first value is in better agreement with the conductivity data for BYZ,[4] it still remains quite low compared with the experimental value of 0.44 eV.

The importance of the O–O separation for the proton diffusion, which we investigate in this paper, was earlier discussed by Kreuer.[24–26] Our data for the BO_6 octahedra in the Zr–OH–Y configuration confirm the results reported in Refs. 25 and 26 that short oxygen separations, which favor proton transfer, and long oxygen separations, which allow rapid bond breaking, correspond to similar free energies of the entire system and, therefore, have similar probabilities of occurring. This flat energy curve favors to what we call chaotic fluctuations in the distances between the O atoms involved in the hydrogen bonding, which is an important step of the proton diffusion mechanism in doped perovskite oxides.

Another important aspect of the conduction mechanism, which was earlier discussed in literature,[25,26] is geometry of the $O-H\cdots O$ hydrogen bonds. It was reported that for most configurations with short O–O separations, the proton was not found between the two oxygens on the edge of the octahedron but outside the BO_6 octahedron as part of a strongly bent hydrogen bond. The reason for this is probably the repulsive interaction between the proton and the highly charged B-site cation, which prevents a linear hydrogen bond from being formed. The analysis of a few transition-state configurations showed that the B–O bonds are somewhat elongated, and the transferring proton was displaced into the edge of the distorted octahedron. Thus an almost linear, short $O-H\cdots O$ configuration is formed.[25,26] Our data also show that the hydrogen bonds on the edges of the BO_6 octahedra are strongly bent. Shortening of the O–O separation leads to less bent $O-H\cdots O$ bonds, but they are still quite far from the linear configuration even at the very short O–O separation, ~2.45 Å (see Table I).

As for the B–O bonds, we find two opposite trends for the distances between the B cation and oxygen atoms involved in the hydrogen bonding. While the $B-O_A$ (acceptor) length increases with shorter O–O separations, the $B-O_D$ (donor) length decreases so that the average B–O distance for these two bonds remains practically same for all O–O separations in the Zr–OH–Y configuration (Table I). This looks plausible because the shorter O–O separation, the more symmetric hydrogen bond, and therefore the more similarity between O_A and O_D. Longer O_D-H distances make the O_D-H bonding weaker which results in shorter $B-O_D$ distances, and vice versa, the shorter $O_A\cdots H$, the stronger corresponding bond and the longer $B-O_A$ distances. These

trends are observed for the corresponding ZrO_6-octahedron in Zr–OH–Zr configuration as well (Table I), but the $B-O_A$ bond increases so dramatically with the shortening of the O–O separation that the average length of $B-O_A$ and $B-O_D$ also increases. The large structure distortion contribution to the free energy arising in this case makes the proton transfer on the O–O edge of the ZrO_6-octahedron in the Zr–OH–Zr configuration unfavorable. Interestingly that the B–H distance decreases with decreasing the O–O separation. This probably occurs due to a stronger screening effect at shorter O–O separations which lowers the Coulomb interaction between the B-cation and proton.

In our and all cited here computational works the proton transfer is found to be the rate-limiting step for the proton transport in BYZ. However, there is disagreement about the proper proton transport mechanism. Based on the analysis of the lattice distortion Münch *et al.*[12] and Gomez *et al.*[11] arrived at a conclusion that only intraoctahedral proton transfer occurs in BYZ, but the energetics obtained in our calculations allows both intra- and interoctahedral proton transfers in BYZ.

IV. SUMMARY AND CONCLUSIONS

A series of quantum mechanical DFT calculations on the $Ba_8Zr_7YHO_{24}$ periodic structure have been carried out to find energy barriers and pathways for the appropriate proton diffusion. Shortening of the H-bonded O–O separation drastically drops the energy barrier for the proton transfer, while the corresponding total energy just moderately increases.

The intraoctahedral proton transfer can occur in the Zr–OH–Y configuration on edges of ZrO_6 octahedra as well as YO_6 octahedra. There is a chance that the interoctahedral proton transfer can also occur in BYZ. More studies are needed to make a firm conclusion.

Based on the results obtained, the atomic level proton diffusion mechanism and possible proton diffusion pathways have been proposed for the BYZ electrolyte. The proton transfer within the double-well hydrogen bond is the rate-limiting step in the proton transport mechanism in BYZ.

The QM results obtained in this work for the proton transfer barriers in BYZ were used in development of a ReaxFF reactive force field which then was successfully employed for molecular dynamics simulations of the diffusion and structural properties of the bulk BYZ phase and grain boundaries.[10]

ACKNOWLEDGMENTS

This work was supported by the U.S. Department of Energy under Grant No. DE-FC26-02NT41631 (program manager Lane Wilson). In addition, some support was provided by DoD Multidisciplinary University Research Initiative (MURI) program administered by the Office of Naval Research under Grant No. N00014-02-1-0665 (program manager Michele Anderson). The facilities of the Materials and Process Simulation Center (MSC) used in this study were established with grants from DURIP-ONR, DURIP-ARO, and NSF-MRI. Additional support for the MSC comes from ONR, ARO, DOE, NSF, NIH, Chevron, Nissan, Dow Corning, Intel, Pfizer, Boehringer-Ingelheim, and Allozyne.

[1] H. Iwahara, H. Uchida, and S. Tanaka, Solid State Ionics **9–10**, 1021 (1983).
[2] H. Iwahara, H. Uchida, K. Ono, and K. Ogaki, J. Electrochem. Soc. **135**, 529 (1988).
[3] K.-D. Kreuer, S. Adams, W. Münch, A. Fuchs, U. Klock, and J. Maier, Solid State Ionics **145**, 295 (2001).
[4] H. G. Bohn and T. Schober, J. Am. Ceram. Soc. **83**, 768 (2000).
[5] S. M. Haile, G. Staneff, and K. H. Ryu, J. Mater. Sci. **36**, 1149 (2001).
[6] W. G. Coors and D. W. Readey, J. Am. Ceram. Soc. **85**, 2637 (2002).
[7] K.-D. Kreuer, Solid State Ionics **125**, 285 (1999).
[8] F. Shimojo, K. Hashino, and H. Okazaki, J. Phys. Soc. Jpn. **66**, 8 (1997).
[9] A. C. T. van Duin, B. V. Merinov, S. S. Jang, and W. A. Goddard III, J. Phys. Chem. **112**, 3133 (2008).
[10] A. C. T. van Duin, B. V. Merinov, S. S. Han, C. O. Dorso, and W. A. Goddard III, J. Phys. Chem. **112**, 11414 (2008).
[11] M. A. Gomez, M. A. Griffin, S. Jindal, K. D. Rule, and V. R. Cooper, J. Chem. Phys. **123**, 094703 (2005).
[12] W. Münch, K.-D. Kreuer, G. Seifert, and J. Maier, Solid State Ionics **136–137**, 183 (2000).
[13] J. P. Perdew, K. Burke, and M. Ernzerhof, Phys. Rev. Lett. **77**, 3865 (1996).
[14] D. M. Ceperley and B. J. Alder, Phys. Rev. Lett. **45**, 566 (1980).
[15] J. P. Perdew and A. Zunger, Phys. Rev. B **23**, 5048 (1981).
[16] P. Schultz, SEQQUEST, Sandia National Laboratories, http://dft.sandia.gov/Quest/; P. J. Feibelman, Phys. Rev. B **35**, 2626 (1987).
[17] C. F. Melius and W. A. Goddard III, Phys. Rev. A **10**, 1528 (1974).
[18] A. Redondo, W. A. Goddard III, and T. C. McGill, Phys. Rev. B **15**, 5038 (1977).
[19] M. E. Björketun, P. G. Sundell, and G. Wahnström, Phys. Rev. B **76**, 054307 (2007).
[20] B. V. Merinov, Solid State Ionics **84**, 89 (1996).
[21] G. Kresse and J. Hafner, Phys. Rev. B **48**, 13115 (1993); G. Kresse and J. Furthmüller, Comput. Mater. Sci. **6**, 15 (1996); Phys. Rev. B **54**, 11169 (1996).
[22] G. Henkelman, B. P. Uberuaga, and H. Jonsson, J. Chem. Phys. **113**, 9901 (2000).
[23] C. T. Chudley and R. J. Elliott, Proc. Phys. Soc. London **77**, 353 (1961).
[24] K. D. Kreuer, A. Fuchs, and J. Maier, Solid State Ionics **77**, 157 (1995).
[25] K. D. Kreuer, Solid State Ionics **136–137**, 149 (2000).
[26] K. D. Kreuer, Annu. Rev. Mater. Res. **33**, 333 (2003).